Asian Journal of Applied Science and Technology (AJAST)
Volume 10, Issue 2, Pages 23-37, April-June 2026

Seismic Amplitudes and Spectral Attributes for Reservoir Characterization and Enhanced Prospect Definition of FUBA Field, Onshore Niger Delta, Nigeria

U. Ochoma[1*]

[1]*Department of Physics, Rivers State University, P.M.B. 5080, Port Harcourt, Nigeria.*
Corresponding Author (U. Ochoma) Email: umaocho@gmail.com[*]

DOI: Under Assignment

Article Received: 22 February 2026 *Article Accepted: 25 April 2026* *Article Published: 28 April 2026*

ABSTRACT

Seismic amplitudes and spectral attributes analysis for reservoir characterization and enhanced prospect definition of Fuba Field, onshore Niger Delta, Nigeria is here presented. Seismic interpretation was carried out using Petrel software. The structural interpretation of seismic data reveal highly synthetic and antithetic faults which are in line with faults trends identified in the Niger Delta. Three distinct horizons were mapped. Reservoir M is found at a shallower depth from 10937 to 10997 ft, reservoir N is found at a depth ranging from 11213 to 11241 ft while reservoir O is found at a deeper depth ranging from 11681 to 11871 ft respectively. By extracting attribute maps of envelope, sweetness, maximum amplitude and RMS (root mean square) amplitude, characterization of the sand units in terms of reservoir geomorphological features, facies distribution and hydrocarbon potential was achieved. The envelope and the sweetness values show similar amplitude characteristics and structure but with varying resolutions. The sweetness value ranges from 0 to 22,500. The high sweetness regions in the seismic data indicate high amplitude which indicates the presence of hydrocarbon-bearing sand units. The maximum amplitude was seen to have bright spot anomalies. These amplitude anomalies served as DHIs (direct hydrocarbon indicators), unravelling the presence and possible hydrocarbon prospective zones. The RMS amplitude values range from 0 to 12,000. The results of spectral decomposition show similar amplitude characteristics and structure with the RMS but with varying resolutions. The spectral attributes indicate areas of low frequency and high amplitude associated with known hydrocarbon zones and meandering channels in the field. At the north-eastern to the south-eastern part and south- western directions, there is high amplitude, an indication of hydrocarbon/gas effect. The results from this study will help in the recovery of more hydrocarbon as by-passed zones and subtle structures are revealed in the area of study.

Keywords: Geomorphological Features; Facies Distribution; Hydrocarbon Potential; Seismic Amplitudes; Sweetness; Spectral Attributes; Envelope; Maximum Amplitude; Niger Delta; Nigeria.

1. Introduction

Reservoir characterization entails identifying, mapping and estimating petrophysical, structural, stratigraphic and geometric reservoir properties for effective development and exploitation of hydrocarbons from well and seismic data (Munyithya, et al., 2020). Seismic amplitude extracted from the seismic reflection data is a measure of the reflection strength governed by the contrast in elastic properties across the geologic interface. The amplitude response of a reflection event across a geologic interface depends on the pore geometry, saturation and pore fluid type, lithology, pressure and depth of burial and has become the most used attribute in reservoir characterization (Hilteman, 2001). Spectral analysis has been one of the significant interpretation methods in seismic analysis because seismic data is non-stationary in nature (Bayowa, et al, 2021). Compared with horizon-based slices in time domain, spectral analysis provides better vertical resolution of various depositional features on frequency slices (Naseer, and Asim, 2018; Tayyab, et al, 2017; Wei et al. 2019).

This study is taken from Fuba Field, Depobelt, Niger Delta, Nigeria. The ultimate deliverable of this study was integrating seismic amplitudes and spectral attributes for improved reservoir characterization and enhanced prospect definition of the area. The major components of this study are: (a) Well Correlation performed in order to determine the continuity of the reservoir sand across the field. (b) Seismic Interpretation which involves well-to-seismic tie, fault mapping, horizon mapping, time surface generation and attributes generation. This aids in

giving more insight into seismic amplitudes and spectral attributes analysis for reservoir characterization and enhanced prospect definition of Fuba field, onshore Niger Delta, Nigeria.

The proposed study area Fuba Field is located in the onshore Niger Delta region. Figure 1 shows the map of the Niger Delta region showing the location of the study area and the base map showing well locations in the study area. The Niger Delta lies between latitudes 4° N and 6° N and longitudes 3° E and 9° E (Whiteman, 1982). The Delta ranks as one of the major oil and gas provinces globally, with an estimated ultimate recovery of 40 billion barrels of oil and 40 trillion cubic feet of gas (Adegoke, et al., 2017). The coastal sedimentary basin of Nigeria has been the scene of three depositional cycles (Short, and Stauble, 1967).

The first began with a marine incursion in the middle Cretaceous and was terminated by a mild folding phase in Santonian time. The second included the growth of a proto-Niger delta during the Late Cretaceous and ended in a major Paleocene marine transgression. The third cycle, from Eocene to Recent, marked the continuous growth of the main Niger delta. A new threefold lithostratigraphic subdivision is introduced for the Niger delta subsurface, comprising an upper sandy Benin Formation, an intervening unit of alternating sandstone and shale named the Agbada Formation, and a lower shaly Akata Formation. These three units extend across the whole delta and each range in age from early Tertiary to Recent. They are related to the present outcrops and environments of deposition. A separate member of the Benin Formation is recognized in the Port Harcourt area. It is Miocene-Recent in age with a minimum thickness of more than 6,000 ft (1829 m) and made up of continental sands and sandstones (>90 %) with few shale intercalations (Horsfall, et al., 2017). Subsurface structures are described as resulting from movement under the influence of gravity and their distribution is related to growth stages of the delta (Ochoma, 2023). Rollover anticlines in front of growth faults form the main objectives of oil exploration, the hydrocarbons being found in sandstone reservoirs of the Agbada Formation.

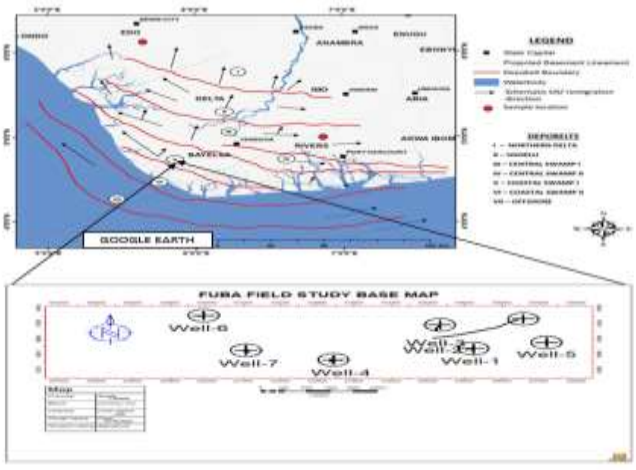

Figure 1. Map of Niger Delta Showing the Study Area and Base Map Showing Well Locations in the Study Area (Source: Google Earth 2026)

1.1. Study Objectives

The objectives of the study include the following:

1) Delineation of reservoir units.

2) Generation of synthetic seismogram and well-to-seismic tie.

3) Generation of time surfaces.

4) Generation of seismic attributes.

5) Generation of spectral attributes.

6) Identification of hydrocarbon prospective areas.

2. Literature

Previous studies have independently demonstrated the effectiveness of seismic reflection amplitudes and spectral attribute analysis as direct hydrocarbon indicators (DHIs), as well as for mapping stratigraphic units, structural features, and evaluating reservoir properties (Ochoma, 2023; Tomasso et al., 2010; Othman et al., 2016; Khan and Masood, 2025; Sofolabo and Nwakanma, 2025). Ochoma (2023) employed variance edge analysis to delineate both prominent and subtle faults within the study area. The results of spectral decomposition revealed zones of low frequency and high amplitude associated with known hydrocarbon accumulations, meandering channels, lobes, and small-scale faults. Similarly, Tomasso et al. (2010) applied spectral re-composition techniques to recover frequencies and their associated amplitudes through an improved inverse formulation. These studies collectively highlight the importance of spectral and amplitude-based seismic attributes in enhancing reservoir characterization and structural interpretation.

Despite their effectiveness, seismic amplitudes are often affected by ambiguities arising from acquisition footprints, processing and imaging errors, surface conditions, and geological factors, which may result in interpretation pitfalls during reservoir characterization if not properly validated (Harilal, 2010; Helal et al., 2015; Rotimi et al., 2010). Validation of amplitude interpretation can be achieved through techniques such as amplitude variation with offset (AVO), shear-wave analysis, or by examining the characteristics of reflection events, including frequency behavior. In this regard, Khan and Masood (2025) proposed an improved spectral decomposition approach known as Continuous Amplitude Phase Spectrum (CAPS), which provides both high-frequency and high time/depth resolution of amplitude and phase spectra. Their study utilized publicly available seismic datasets from the Stratton and Penobscot fields, alongside well logs from the Penobscot field, including gamma-ray, sonic, density, and neutron porosity logs. The features derived from CAPS decomposition showed strong agreement with previously reported findings, demonstrating the reliability of the technique for reservoir interpretation.

Sofolabo and Nwakanma (2025) investigated a field within the Central Depobelt sedimentary basin of the Niger Delta, Nigeria, to identify potential structural and stratigraphic controls using surface seismic attributes. Several attributes, including reflection intensity, RMS amplitude, time gain, trace AGC (Automatic Gain Control), sweetness, envelope, instantaneous frequency, instantaneous phase, quadrature amplitude, ant tracking, dip deviation, gradient magnitude, local structural dip, chaos, iso-frequency, and local flatness, were applied in the interpretation of the 3D seismic cube and generated time and depth surface maps. The results revealed moderate to high sweetness regions (sweet spots), acoustic impedance contrasts indicating lithologic changes and possible hydrocarbon presence, as well as enhanced fault and fracture signatures through variance, dip deviation, gradient

magnitude, and ant-tracking attributes. The study validated lithology discrimination using elastic rock properties from well logs and demonstrated the effectiveness of seismic attributes in identifying and unmasking hidden reservoir features. Consequently, the findings suggest that accurate hydrocarbon exploration and production depend on proper reservoir characterization in terms of fluid properties and lithology using seismic-derived attributes. Therefore, integrating seismic amplitudes with spectral attributes can significantly improve interpretation confidence and increase the success rate of drilling operations.

3. Methodology

3.1. Well-to-Seismic Ties

Well correlation is the first stage of the pre-interpretation process. The process of well correlation involves lithologic description, picking top and base of sand bodies, fluid discrimination, and linking these properties from one well to another based on similarity in trends. In the Niger Delta, the predominant lithologies are sands and shales; therefore, the gamma ray log is commonly used to discriminate between these lithologies in the subsurface. Correlation of reservoir sands was achieved using the picked tops and bases of the reservoir sands. The correlation process was possible based on similarities in the behavior and shapes of the gamma ray log responses. In addition, the thickness of the shale bodies overlying and underlying the sand body was considered during the correlation process. After defining the lithologies, the resistivity log was used to discriminate the type of fluid occurring within the pore spaces of the rocks.

Accurate well correlation is essential because it provides the framework for reliable reservoir characterization and seismic interpretation. The integration of well logs with seismic data helps in reducing interpretation uncertainty and improves the understanding of subsurface stratigraphic and structural relationships. Furthermore, well-to-seismic ties establish a direct relationship between geological information obtained from wells and reflection events observed on seismic sections. This integration enhances confidence in horizon identification, fault delineation, and reservoir mapping.

In addition to lithologic and fluid interpretation, well correlation also assists in identifying lateral continuity and heterogeneity within reservoir units. Variations in log signatures across wells may indicate depositional changes, compartmentalization, or the influence of structural deformation within the reservoir interval. The use of multiple well logs during correlation provides a more comprehensive understanding of reservoir geometry and petrophysical characteristics. This approach improves the reliability of stratigraphic interpretation and supports the identification of potential hydrocarbon-bearing zones. Consequently, integrating well data with seismic information forms a robust foundation for detailed structural and stratigraphic analysis within the study area.

There are five basic steps involved in seismic interpretation relevant to this study, namely: well-to-seismic ties, fault mapping, horizon mapping, time surface generation and attribute generation. Well-to-seismic tie is a process that enables the visualization of well information on seismic data. For this process to be achieved, the following are basic requirements: checkshot data, sonic log, density log and a wavelet. The sonic log, which is the reciprocal of velocity, was calibrated using the checkshot data. The calibration process is necessary in order to improve the

quality of the sonic log because the sonic log is prone to washouts and other wellbore-related issues. The result of calibrating the sonic log with the checkshot data produces a new log known as the calibrated sonic log.

The calibrated sonic log was used together with the density log to generate an Acoustic Impedance (AI) log. The acoustic impedance log was calculated for each rock layer. The next step involved generating the Reflection Coefficient (RC) log, which was computed using the AI log. The RC log generated was then convolved with a wavelet to produce a synthetic seismogram comparable with the seismic data. The statistical wavelet utilized for convolution was extracted from the seismic dataset. Synthetic seismograms were generated for all wells that contained checkshot, density, and sonic logs. The reflections on the synthetic seismograms were matched with the reflections observed on the seismic sections to establish accurate well-to-seismic ties. The mathematical expressions governing the workflow are presented below:

$$AI = \rho v \quad (1)$$

$$RC = \frac{\rho_2 v_2 - \rho_1 v_1}{\rho_2 v_2 + \rho_1 v_1} \quad (2)$$

$$\textit{Synthetic Seismogram} = \frac{\rho_2 v_2 - \rho_1 v_1}{\rho_2 v_2 + \rho_1 v_1} * wavelet \quad (3)$$

Where ρ= Density, v =Velocity, AI= Acoustic impedance and, RC= Reflection coefficient.

Faults were identified as discontinuities or breaks within the seismic reflections. Fault mapping was carried out along both inline and crossline directions. Horizons are continuous lateral reflection events truncated by fault lines; therefore, horizon interpretation was also conducted along both inline and crossline directions. At the completion of horizon mapping, a seed grid was generated, which served as the input for time surface generation. The generated time surfaces provided the structural framework for subsequent seismic attribute extraction and reservoir characterization.

3.2. Determination of Envelope

Envelope attribute or reflection strength displays acoustically strong events on both negative and positive events. It is calculated from the complex trace of seismic signal used to highlight the main seismic features. It represents the instantaneous energy of the signal and is proportional in its magnitude to the reflection coefficient.

3.3. Determination of Sweetness

Sweetness involves the implementation of envelopes and instantaneous frequency that are combined. Mathematically, it is expressed as

$$S(t) = \frac{\alpha(t)}{\sqrt{f_\alpha(t)}} \quad (4)$$

where $S(t)$ = Sweetness, $\alpha(t)$ =Envelope, $f_\alpha(t)$ = instantaneous frequency.

Sweetness is used for the identification of features where the total energy signatures change in the seismic data.

3.4. Determination of Maximum Amplitude

Amplitude is the deviation a wave from zero crossing. Maximum positive amplitude is referred to as peak value. The maximum amplitude attribute computation in Petrel software makes use of the inbuilt formula:

$$y = A\sin(\omega t + \phi) \qquad (5)$$

where $A =$ Amplitude of the seismic wave, $\phi =$ Phase of the seismic wave, $\omega =$ Angular frequency of the seismic wave and $t =$ time period.

3.5. Determination of Root Mean Square (RMS) Amplitude

Root mean square (RMS) amplitude is used to obtain a scaled estimate of seismic trace envelope. It is obtained in the software by sliding a tapered window of N samples as the square root of the sum of all the trace value x squared. The RMS attribute computation in Petrel software makes use of the inbuilt formula:

$$X_{rms} = \sqrt{\frac{1}{N}\sum_{n=1}^{N} w_n x_n^2} \qquad (6)$$

where $X_{rms} =$ root mean square amplitude, $w_n =$ window values, $N =$ number of samples in the window, $x =$ trace value.

3.6. Spectral Decomposition

Spectral decomposition is a frequency attribute. It involves separating and classifying seismic events within each trace based on their frequency content. Each 1D trace was decomposed from the time domain into its corresponding 2D representation in the time-frequency domain using algorithms. Once each trace was transformed into the time-frequency domain, a band-pass filter was applied to view the amplitude of seismic data at different frequencies.

The short-time Fourier transform (STFT) spectrogram which is the squared modulus of the STFT and the spectral energy density is defined as (Cohen, 1989)

$$SP_s(t, f) = /\int_{-\infty}^{\infty} s(\tau)h(\tau - t)e^{-j2\pi f\tau}d\tau /^2 \qquad (7)$$

Where, $h(\tau - t) =$ the window function, $s(\tau) =$ the signal, $SP_s =$ the short-time Fourier transform

$j =$ the imaginary unit, $\tau =$ the time delay.

The relationships between the amplitude spectrum ($A(\omega)$) and the phase spectrum ($\gamma(\omega)$) of the estimated transformed signals are presented in equations 8 and 9

$$/A(\omega^T)/ = \sqrt{A_r + A_i} \qquad (8)$$

$$\gamma(\omega) = \mathrm{Tan}^{-1}[\frac{A_i}{A_r}] \qquad (9)$$

Where, A_r = real part of $A(\omega^T)$, A_i = imaginary part of $A(\omega^T)$, ω =frequency, T = transform of the signal, $A(\omega^T)$ = amplitude of transformed trace at frequency ω.

4. Results and Discussions

4.1. Reservoir Identification and Correlation

The results for lithology and reservoir identification are presented in (Figure 2). A total of four sand bodies (L, M, N and O) were identified and correlated across all seven wells in the field. Three reservoir sands were selected for the purpose of this study (M, N and O). The resistivity logs which reveal the presence of hydrocarbons were used to identify the hydrocarbon bearing sands. On Figure 2, the sands are coloured yellow while shales are grey in colour. Figure 3 shows the checkshot quality of Well-1 utilized for well-to-seismic tie. The results for well-to-seismic tie conducted on FUBA field using density log, sonic log and checkshot of Well-1 is presented in Figure 4. An extended white 2 wavelet was used to give a near perfect match between the seismic and synthetic seismogram.

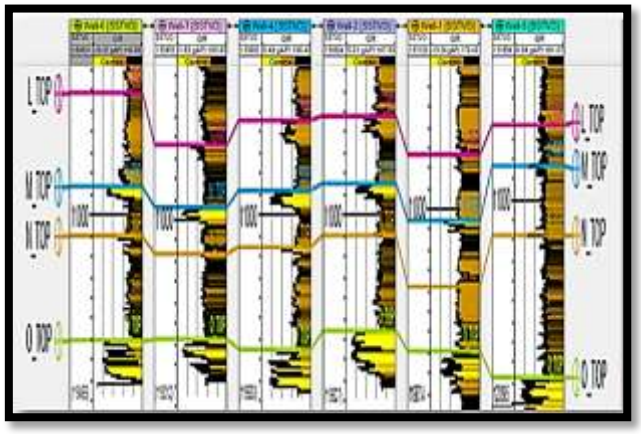

Figure 2. Identification of Correlation of Reservoirs L, M, N and O Across Fuba Field

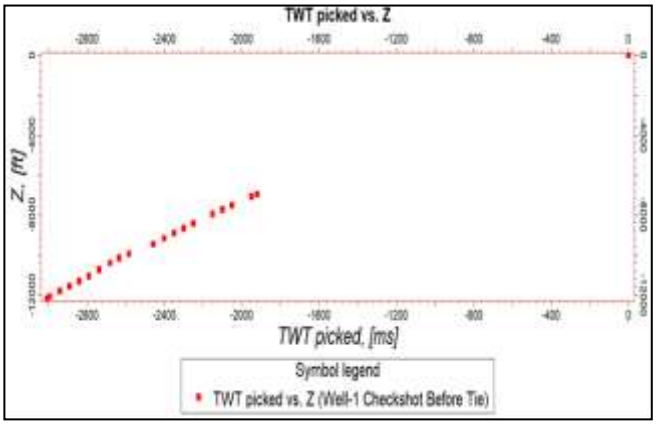

Figure 3. Checkshot Quality of Well-1, Showing no out-liers, Utilized for Well-to-seismic Tie

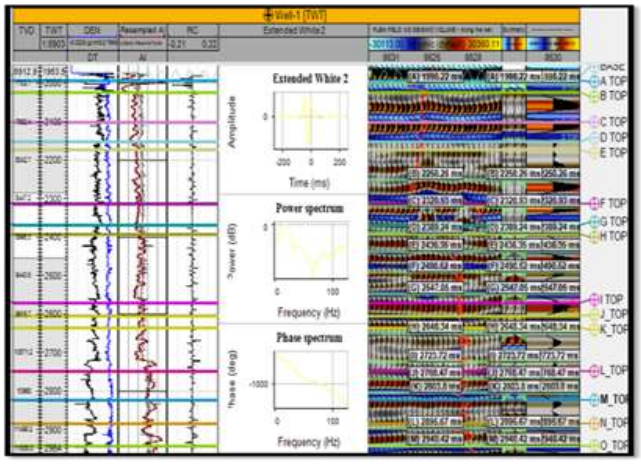

Figure 4. Synthetic Seismogram Generation and Interpreted Well-to-seismic Tie Conducted for Fuba Field Using Well-1 Checkshot.

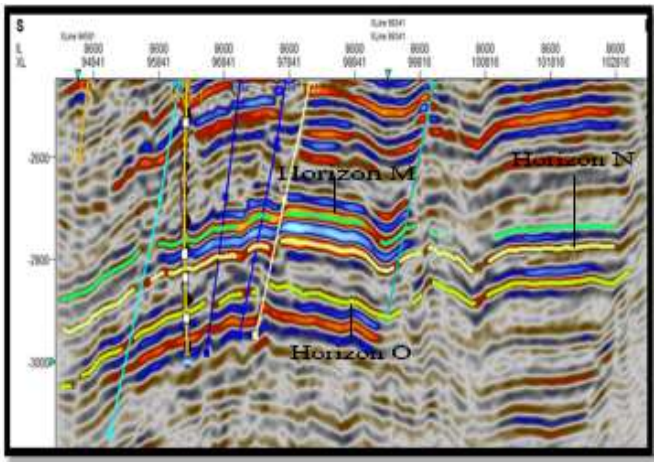

Figure 5. Faults and Horizons M, Nand O Along Seismic Inline Section.

Asian Journal of Applied Science and Technology (AJAST)
Volume 10, Issue 2, Pages 23-37, April-June 2026

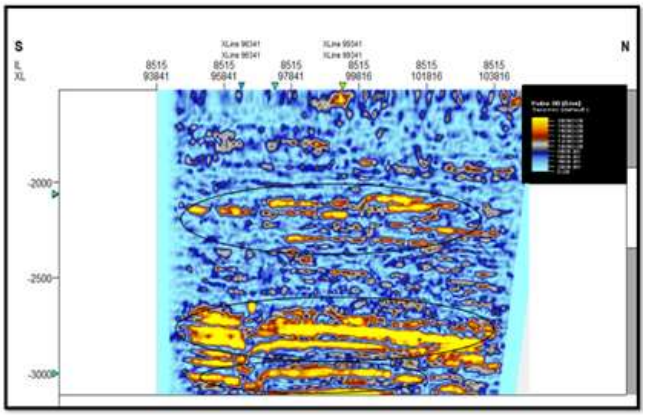

Figure 6. Envelope inline 8515 Showing High Amplitude Anomalies Exhibiting the Signature of a Channel Sand Saturated with Hydrocarbon.

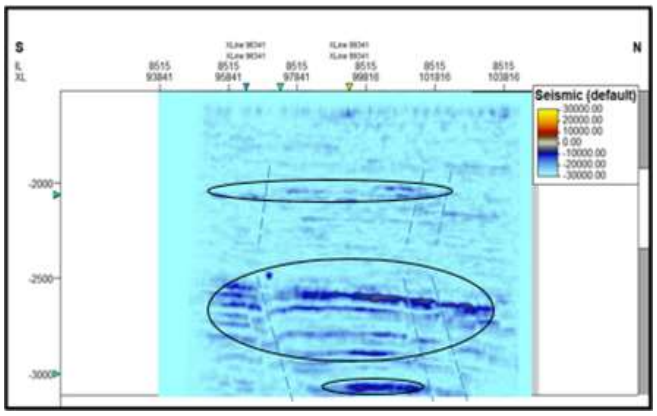

Figure 7. Sweetness Inline 8515 Showing High Amplitude Anomalies Exhibiting the Signature of a Channel Sand Saturated with Hydrocarbon

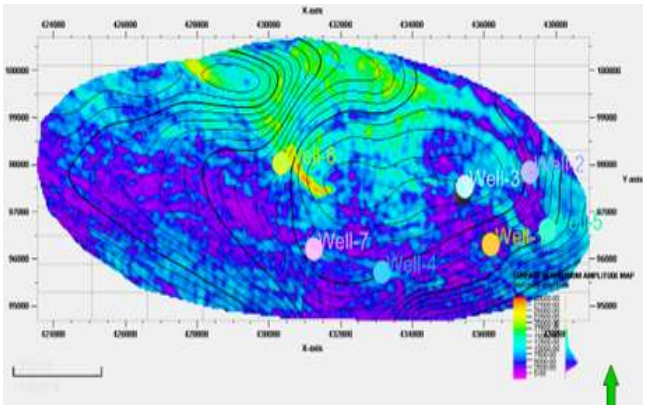

Figure 8. Maximum Amplitude Map for Reservoir Surface M Showing Strong Amplitude Anomalies Exist at the Central Part of the Field and Parts of Northeast, Northwest, Southwest and Southeast Sections.

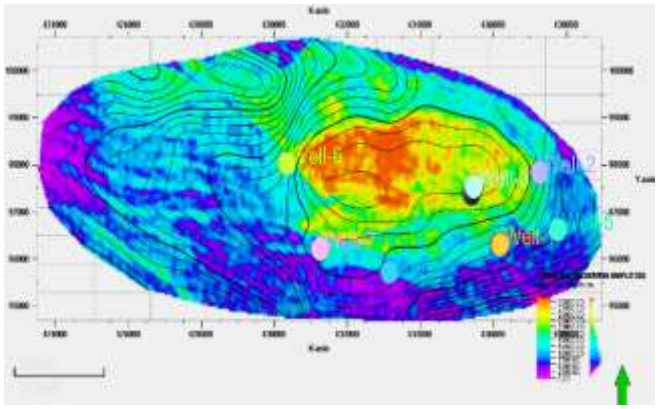

Figure 9. Maximum Amplitude Map for Reservoir Surface N Showing Strong Amplitude Anomalies Exist at the Central Part of the Field and Parts of Northeast, Northwest, Southwest and Southeast Sections.

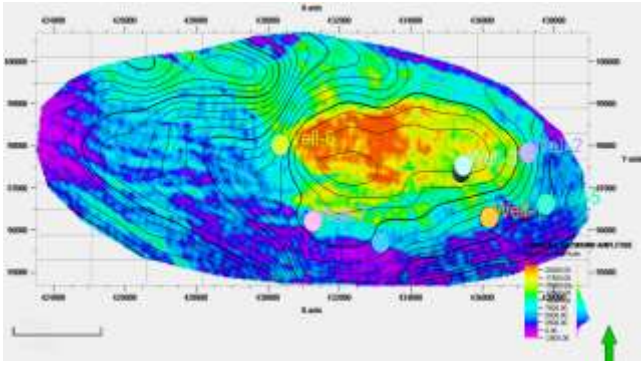

Figure 10. Maximum Amplitude Map for Reservoir Surface O Showing Strong Amplitude Anomalies Exist at the Central Part of the Field and Parts of Northeast, Northwest, Southwest and Southeast Sections.

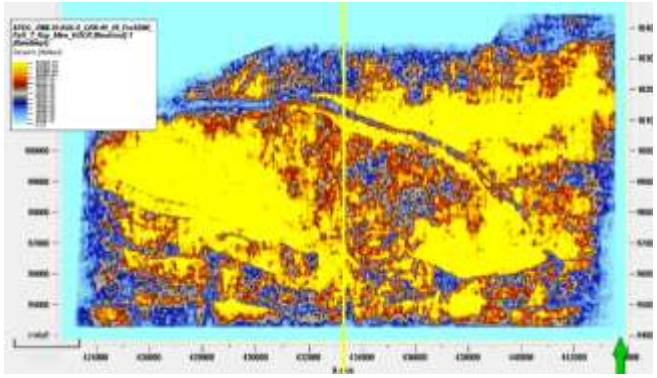

Figure 11. 3D Volume RMS Time Slice at Z=2060 Indicating RMS Amplitude

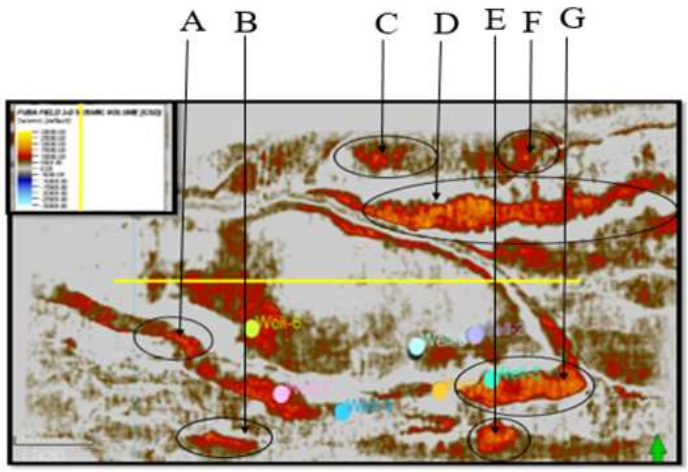

Figure 12. The General Spectral Decomposition Volume at Frequency of 35Hz Indicating the Prospect Zones A, B, C, D, E, F and G.

4.2. Fault and Horizon Interpretation

The results for the interpreted faults in Fuba field are presented in Figure 5 shows both synthetic and antithetic faults interpreted along seismic inlines. Faults are more visible along the inline direction because this direction reveals the true dip position of geologic structures. The variance time slice was used to validate the interpreted faults. All interpreted faults are normal synthetic and antithetic faults. A total of thirty-six faults were interpreted across the entire seismic data. Of the 36 interpreted faults, only F1 (synthetic fault) and F4 (antithetic fault) faults are regional, running from the top to bottom across the field. Hence, these faults play significant roles in trap formation at the upper, middle and lower sections of the field.

The results for the interpreted seismic horizons (Horizons M, N and O) are also presented in Figure 5. On these horizons, the fault polygons were generated and eliminated. The horizons were used as inputs for the generation of reservoir time surfaces. The reservoir time surfaces (M, N and O reservoirs) reveal that the reservoir structure is a collapsed crest, bounded by two regional faults (F1 and F4). Reservoir M, N and O time surfaces are truncated by two bounding faults and three minor inter-reservoir faults. The fault supported collapsed crestal structures are the closures identified on reservoir M, N and O reservoir surfaces respectively. The similarity in structure on reservoir M, N and O reveals that the field is structurally controlled by faults. Reservoir M is found at a shallower depth from 10937 to 10997 ft, reservoir N is found at a depth ranging from 11213 to 11241 ft while reservoir O is found at a deeper depth ranging from 11681 to 11871 ft respectively.

4.3. Seismic Attributes

A series of seismic attributes such as envelope, sweetness, maximum amplitude and RMS (Root Mean Square) amplitude were generated in Petrel software interface to investigate potential structural and stratigraphic controls within the study area.

Figure 6 represents the envelope while Figure 7 represents the sweetness values of the seismic data. They show similar amplitude characteristics and structure but with varying resolutions. High-amplitude anomalies exhibiting

the signature of a channel sand saturated with hydrocarbons were mapped in each attribute map (Okocha, and Atakpo, 2017; Kosen, 2014). Sweetness attribute is the more robust with brighter amplitudes than the envelop attribute. This is due to the composite nature of sweetness attribute (a function of envelop and frequency) and its less sensitivity to noise compared to the envelope attribute. The sweetness value ranges from 0 (blue) to 22,500 (yellow). High sweetness values may be attributed to both high amplitude and low frequency while low sweetness value is as a result of low amplitude and high frequency in the seismic volume.

The maximum amplitude maps generated for the studied surfaces (surface M, N and O) showed that strong amplitude anomalies exist at the central part of the field and parts of northeast, northwest, southwest and southeast sections (Figures 8-10). The parts of the field where these strong amplitude anomalies were observed corresponds to the observed anticlinal structure in the field. Other parts of the field where the amplitude anomalies were observed also correspond to the identified structural closures found in the field. Results indicate that strong amplitude anomalies are structurally controlled as they are seen occurring near faults on structural maps. The maximum amplitude maps generated for the studied surfaces presented were seen to have bright spot anomalies, which are likely associated with of facies and/or fluid content (Raef, et al, 2016). In addition, these anomalies are seen on structural high, which suggested prospect conformity with regional structural high. The result is similar to that of Ochoma, 2023.

The 3D volume RMS time slice at Z=2060 indicating RMS amplitude is presented in Figure 11. The RMS amplitude values range from 0 (purple) to 12,000 (yellow). The red-yellowish colour represents hydrocarbon sands. Some of these hydrocarbon sands were not detected in the original seismic section. The observed changes may be due to changes in lithology or fluid content.

RMS amplitude is similar to reflection strength and it is used in seismic exploration for delineating bright spots and amplitude anomalies (Fozoa, et al, 2018; Opara, and Osaki, 2018). The high amplitude in the seismic data conforms to the structures and confirms the presence of hydrocarbon (Ajisafe, and Ako, 2013). The high amplitude ranges from light blue to red and yellow coloration. Root mean square amplitude is used as a good indicator of the presence of hydrocarbon in seismic data.

4.4. Spectral Decomposition

The general spectral decomposition was done at a frequency of 35Hz for the seismic. Figure 12 is the seismic volume obtained for the general spectral decomposition. It shows similar amplitude characteristics and structure with the RMS Volume but with varying resolutions. Figure 12 illustrates RGB (Red-Green-Blue) blend of the higher resolution of the frequency of 35Hz. The RGB colour blend effect gives a better understanding of the reservoirs geology. The colour blend is spectral balancing which recompense for wavelet and energy loss. The figure showed a complex meandering system and other less winding channels which are discontinuous and difficult to resolve on the seismic. The RGB colour blending slices revealed more hidden structures compared with what is observed in the time structural map. In this figure, the areas in red color indicate areas of low frequency and high amplitude associated with known hydrocarbon zones (Ehirim, and Akpan, 2017**)** and when one colour is dominating, it showed that the frequency is dominating at that point. It revealed the geometry of the channels and

other fewer sinusoidal channels. The channels are displayed with bright colouration which contains multiple frequencies as observed within the low frequency and high amplitude (indicated in black circles in Figure 12). The wells are located on and along the channel sands in the field. At the north-eastern to the south-eastern part and south- western directions, there is high amplitude, an indication of hydrocarbon/gas effect. This is considered a bypassed prospect in agreement with the results of the seismic amplitudes. This confirms the possibility of the prospects for hydrocarbon exploitation; the portions of the field are where the thin beds are. This is very important in hydrocarbon exploration wells. The amplitude response which is dominated by blue colour is high frequency. At parts where there's a change in colour to brownish, it showed thickening up of the reflectors and greater contribution from the lower frequencies. There are colour changes in the channel system which could be indicative of changes in lithology.

5. Conclusion and Future Recommendations

A total of four sand bodies (L, M, N and O) were identified and correlated across all seven wells in the field. Three horizons were selected for the study (M, N and O). All interpreted faults are normal synthetic and antithetic faults which are in line with faults trends identified in the Niger Delta. A total of thirty-six faults were interpreted across the entire seismic data. Of the thirty-six interpreted faults, only F1 (synthetic fault) and F4 (antithetic fault) faults are regional, running from the top to bottom across the field. Hence, these faults play significant roles in trap formation at the upper, middle and lower sections of the field. Fault and horizon interpretation revealed that closures found on M, N and O reservoirs are collapsed crestal structures bounded by the two major faults. Reservoir M is found at a shallower depth from 10937 to 10997 ft, reservoir N is found at a depth ranging from 11213 to 11241 ft while reservoir O is found at a deeper depth ranging from 11681 to 11871 ft respectively. By extracting attribute maps of envelope, sweetness, maximum amplitude and RMS amplitude, characterization of the sand units in terms of reservoir hydrocarbon potential was achieved. The envelope and sweetness values show similar amplitude characteristics and structure but with varying resolutions. The sweetness value ranges from 0 to 22,500. The high sweetness regions in the seismic data indicate high amplitude which indicates the presence of hydrocarbon-bearing sand units. The maximum amplitude results highlighted the hydrocarbon zones. The maximum amplitude maps were seen to have bright spot anomalies. These amplitude anomalies served as DHIs (direct hydrocarbon indicators), unravelling the presence and possible hydrocarbon prospective zones. The RMS amplitude values range from 0 to 12,000. The results of spectral decomposition show similar amplitude characteristics and structure with the RMS volume but with varying resolutions. The spectral attributes indicate areas of low frequency and high amplitude associated with known hydrocarbon zones and meandering channels in the field. At the north-eastern to the south-eastern part and south- western directions, there is high amplitude, an indication of hydrocarbon/gas effect. This is considered a by-passed prospect in agreement with the results of the seismic amplitudes. This confirms the possibility of the prospects for hydrocarbon exploitation; the portions of the field are where the thin beds are. This is very important in hydrocarbon exploration wells. The study has demonstrated that the application of seismic attributes, which offers insight on hydrocarbon presence and distribution of reservoir sand, could help unravel prospective intervals where there are no well controls. Hydrocarbon exploration and development risks can be reduced greatly with the outcome of seismic attributes

extraction and analysis. The following are some future suggestions (i) Careful quality control of the updated velocities using existing horizons should be performed so that the resulting velocity maps can be used for accurate depth conversion. (ii) Fault seal analysis should be carried out to confirm that the suspected trapping faults are not leaking in which case they serve as conduits for hydrocarbon migrations rather than lateral barriers to hydrocarbon escape. (iii) Studies should be done on the mapping of thin sandstone reservoirs in the study area. (iv) Further work is recommended to be concentrated on the identified exploitable part of the field with the intention to upgrade the area into drillable prospect by estimating its reserve. (v) Geostatistics should be done to predict reservoirs properties from areas under well control to the prospect areas.

Declarations

Source of Funding

This study did not receive any grant from funding agencies in the public, commercial, or not-for-profit sectors.

Competing Interests Statement

The author declares no competing financial, professional, or personal interest.

Consent for Publication

The author declares that she consented to the publication of this study.

Author's Contribution

The author declares that she carried out the study.

Informed Consent

Not applicable.

Availability of Data and Material

The data and material used for this study was made available by Shell Petroleum Development Company of Nigeria (SPDC), Port Harcourt Nigeria.

Institutional Review Board Statement

Not applicable.

Ethical Approval

Not applicable.

Acknowledgements

The author is grateful to Shell Petroleum Development Company of Nigeria (SPDC), Port Harcourt Nigeria for the release of the academic data for the purpose of this study.

Declaration of Artificial Intelligence

The author declares that she did not use artificial intelligence during the course of this study.

References

[1] Munyithya, M., Ehirim, N.C., Dagogo, T., & K'orowe, M.O. (2020). Seismic amplitudes and spectral attribute analysis in reservoir characterisation, 'MUN' onshore Niger Delta field. Journal of Petroleum Exploration and Production Technology, 10: 2257–2267.

[2] Hilteman, F.J. (2001). Seismic amplitude interpretation. SEG/EAGE Distinguished Instructor Course No. 4.

[3] Bayowa, G.O., Adagunodo, A.T., Oshonaiye, O.A., & Boluwade, S.B. (2021). Mapping of thin sandstone reservoirs in Bisol Field, Niger Delta, Nigeria using spectral decomposition technique. Geodesy and Geodynamics, 12: 54–64.

[4] Naseer, M.T., & Asim, S. (2018). Characterization of shallow-marine reservoirs of Lower Eocene carbonates, Pakistan: Continuous wavelet transforms-based spectral decomposition. Journal of Natural Gas Science and Engineering, 56: 629–649.

[5] Tayyab, M.N., Asim, S., Siddiqui, M.M., Naeem, M., Solange, S.H., & Babar, F.K. (2017). Seismic attributes application to evaluate the Goru clastics of Indus Basin, Pakistan. Arabian Journal of Geosciences, 10(7): 158.

[6] Wei, L., Dali, Y., Wenfeng, W., Wurong, W., Shenghe, W., Jian, L., & Depo, C. (2019). Fusing multiple frequency-decomposed seismic attributes with machine learning for thickness prediction and sedimentary facies interpretation in fluvial reservoirs. Journal of Petroleum Science and Engineering, 177: 1087–1102.

[7] Google (2018). Map of Niger Delta region showing the depo belts. Google Earth. https://www.google.com/earth/.

[8] Ochoma, U. (2023). Spectral attributes in onshore Fuba Field Niger-Delta, Nigeria, using 3-D seismic time-lapse data. Mediterranean Journal of Basic and Applied Sciences, 7(2): 103–115.

[9] Ochoma, U. (2023). Application of time-frequency decomposition and seismic attributes for stratigraphic interpretation of thin reservoirs in onshore Fuba Field Niger-Delta, Nigeria. Irish Interdisciplinary Journal of Science & Research, 7(2): 84–95.

[10] Tomasso, M., Bouroullec, R., & Pyles, D.R. (2010). The use of spectral recomposition in tailored forward seismic modelling of outcrop analogs. AAPG Bulletin, 94: 457–474.

[11] Othman, A.A.A., Fathy, M., & Maher, A. (2016). Use of spectral decomposition technique for delineation of channels for solar gas discovery, offshore West Nile Delta, Egypt. Egyptian Journal of Petroleum, 25: 45–51.

[12] Harilal, S.K.B. (2010). Pitfalls in seismic amplitude interpretation: Lessons from Oligocene channel sandstones. The Leading Edge, 29(4): 384–390.

[13] Helal, A., Farag, K.S.I., & Shihataa, M.I. (2015). Unconventional seismic interpretation workflow to enhance seismic attributes results and extract geobodies at Gulf of Mexico case study. Egyptian Journal of Geology, 59: 1–14.

[14] Rotimi, O.J., Ameloko, A.A., & Adeoye, O.T. (2010). Application of 3-D structural interpretation and seismic attributes analysis to hydrocarbon prospecting over X-field, Niger Delta. International Journal of Basic and Applied Science IJBAS-IJENS, 10(4): 28–40.

[15] Khan, M.M., & Masood, F. (2025). Spectral-derived attributes analysis and interpretation using enhanced spectral decomposition method – A case study of Penobscot and Stratton Fields. Pakistan Journal of Engineering Technology and Science, 13(2): 33–43.

[16] Sofolabo, A.O., & Nwakanma, A. (2025). Seismic attributes for reservoir characterization of a field, central depobelt sedimentary basin of Niger Delta: A qualitative interpretation. Journal of Geography, Environment and Earth Science International, 29(4): 1–21.

[17] Whiteman, A. (1982). Nigeria: Its petroleum ecology resources and potential. Graham and Trotman, London.

[18] Adegoke, O.S., Oyebamiji, A.S., Edet, J.J., Osterloff, P.L., & Ulu, O.K. (2017). Cenozoic foraminifera and calcareous nannofossil biostratigraphy of the Niger Delta. Elsevier, Cathleen Sether, United States.

[19] Short, K.C., & Stable, A.J. (1967). Outline of geology of Niger Delta. Bulletin of American Association of Petroleum Geologists, 51(5): 761–779.

[20] Horsfall, O.I., Uko, E.D., Tamunoberetonari, I., & Omubo-Pepple, V.B. (2017). Rock-physics and seismic-inversion based reservoir characterization of AKOS Field, coastal swamp depobelt, Niger Delta, Nigeria. IOSR Journal of Applied Geology and Geophysics, 5(4): 59–67.

[21] Ochoma, U. (2023). The subsurface structures in onshore Fuba Field Niger-Delta, Nigeria, using 3-D seismic time-lapse data. Mediterranean Journal of Basic and Applied Sciences, 7(2): 116–125.

[22] Cohen, L. (1989). Time-frequency distributions – A review. Proceedings of the IEEE, Pages 941–981.

[23] Okocha, F.O., & Atakpo, E. (2017). Effect of hydrocarbon production on reflection amplitude properties of reservoirs—A case of Kov Field, Niger Delta, Nigeria. Arabian Journal of Geosciences, 10(17): 380.

[24] Kosen, S. (2014). Enhancing geological interpretation with seismic attributes in Gulf of Thailand. B.Sc. Report, Chula Long University, Thailand, Pages 42.

[25] Raef, A.E., Meek, T.N., & Totten, M.W. (2016). Applications of 3-D seismic attribute analysis in hydrocarbon prospect identification and evaluation: Verification and validation based on fluvial palaeochannel cross-sectional geometry and sinuosity, Ness County, Kansas, USA. Marine and Petroleum Geology, 73: 21–35.

[26] Ochoma, U. (2023). Application of 3-D seismic attributes analysis for hydrocarbon prospectivity in onshore Fuba Field, Niger Delta, Nigeria. Asian Journal of Basic Science & Research, 5(2): 83–96.

[27] Fozao, K.F., Fotso, L., Djieto-Lordon, A., & Mbeleg, M. (2018). Hydrocarbon inventory of the eastern part of the Rio Del Rey Basin using seismic attributes. Journal of Petroleum Exploration and Production Technology, 8: 655–665.

[28] Opara, A.I., & Osaki, L.J. (2018). 3-D seismic attribute analysis for enhanced prospect definition of "Opu Field", coastal swamp depo belt Niger Delta, Nigeria. Journal of Applied Science, 18: 86–102.

[29] Ajisafe, Y.C., & Ako, B.D. (2013). 3-D seismic attributes for reservoir characterization of 'Y' Field, Niger Delta, Nigeria. IOSR Journal of Applied Geology and Geophysics, 1: 23–31.

[30] Ehirim, C.N., & Akpan, A.S. (2017). Continuous wavelet transforms based spectral decomposition of 3D seismic data for reservoir characterization in Oyi Field, South East Niger Delta. American Journal of Applied Science, 14(8): 766–771.